San Jose State University

# SJSU ScholarWorks

10-2022

# Large Eddy Simulations of Wind Shear from Passing Vehicles Under a Freeway Overpass

Hamid Rahai
*California State University, Long Beach*

Assma Begum
*California State University, Long Beach*

# SJSU SAN JOSÉ STATE UNIVERSITY

## MTI MINETA TRANSPORTATION INSTITUTE

# Large Eddy Simulations of Wind Shear from Passing Vehicles Under a Freeway Overpass

Hamid Rahai, PhD

Assma Begum, MS

## CSUTC California State University Transportation Consortium

CALIFORNIA STATE UNIVERSITY
**LONG BEACH**

# Mineta Transportation Institute

Founded in 1991, the Mineta Transportation Institute (MTI), an organized research and training unit in partnership with the Lucas College and Graduate School of Business at San José State University (SJSU), increases mobility for all by improving the safety, efficiency, accessibility, and convenience of our nation's transportation system. Through research, education, workforce development, and technology transfer, we help create a connected world. MTI leads the Mineta Consortium for Transportation Mobility (MCTM) funded by the U.S. Department of Transportation and the California State University Transportation Consortium (CSUTC) funded by the State of California through Senate Bill 1. MTI focuses on three primary responsibilities:

### Research

MTI conducts multi-disciplinary research focused on surface transportation that contributes to effective decision making. Research areas include: active transportation; planning and policy; security and counterterrorism; sustainable transportation and land use; transit and passenger rail; transportation engineering; transportation finance; transportation technology; and workforce and labor. MTI research publications undergo expert peer review to ensure the quality of the research.

### Education and Workforce

To ensure the efficient movement of people and products, we must prepare a new cohort of transportation professionals who are ready to lead a more diverse, inclusive, and equitable transportation industry. To help achieve this, MTI sponsors a suite of workforce development and education opportunities. The Institute supports educational programs offered by the Lucas Graduate School of Business: a Master of Science in Transportation Management, plus graduate certificates that include High-Speed and Intercity Rail Management and Transportation Security Management. These flexible programs offer live online classes so that working transportation professionals can pursue an advanced degree regardless of their location.

### Information and Technology Transfer

MTI utilizes a diverse array of dissemination methods and media to ensure research results reach those responsible for managing change. These methods include publication, seminars, workshops, websites, social media, webinars, and other technology transfer mechanisms. Additionally, MTI promotes the availability of completed research to professional organizations and works to integrate the research findings into the graduate education program. MTI's extensive collection of transportation-related publications is integrated into San José State University's world-class Martin Luther King, Jr. Library.

_____

Report 22-43

# Large Eddy Simulations of Wind Shear from Passing Vehicles Under a Freeway Overpass

Hamid Rahai, Ph.D.

Assma Begum, M.S.

October 2022

# TECHNICAL REPORT
# DOCUMENTATION PAGE

| 1. Report No.<br>22-43 | 2. Government Accession No. | 3. Recipient's Catalog No. |
|---|---|---|
| 4. Title and Subtitle<br>Large-Eddy Simulations of Wind Shear from Passing Vehicles Under a Freeway Overpass | | 5. Report Date<br>October 2022 |
| | | 6. Performing Organization Code |
| 7. Authors<br>Hamid Rahai, Ph.D.<br>Assma Begum, M.S. | | 8. Performing Organization Report<br>CA-MTI-2145 |
| 9. Performing Organization Name and Address<br>Mineta Transportation Institute<br>College of Business<br>San José State University<br>San José, CA 95192-0219 | | 10. Work Unit No. |
| | | 11. Contract or Grant No.<br>ZSB12017-SJAUX |
| 12. Sponsoring Agency Name and Address<br>State of California SB1 2017/2018<br>Trustees of the California State University<br>Sponsored Programs Administration 401<br>Golden Shore, 5th<br>Long Beach, CA 90802 | | 13. Type of Report and Period Covered |
| | | 14. Sponsoring Agency Code |
| 15. Supplemental Notes | | |

**16. Abstract**
California is moving toward a 100% clean energy future, and expanded wind energy will be a major component of the state's future energy portfolio. Innovations in wind energy resources will move California closer to achieving its goal. To gain a better understanding of transient pressure and the wind shear generated at the bridge poles from passing vehicles, this study performed large-eddy simulations of a vehicle (also called an Ahmed body) moving under a freeway overpass at a distance of 0.75 w (width) from the bridge poles. Results include transient contours of mean velocity, turbulent kinetic energy, vorticity, and pressure around the vehicle and at the bridge poles at different time steps. Additionally, results indicate the vehicle's base pressure changes with time, indicating the impact of the poles' constraints on the vehicle's drag. On the bridge poles, the location of the stagnation point changes with the passing of the vehicle, and the poles experience a transient load, with the peak load associated with the passage of the vehicle's leading edge. The transient wind generated between the poles is mostly due to the vehicle's front and decreases with the passing of the vehicle. The pressure at this location oscillates between a peak positive and a peak negative, generating a force potential for possible electric power generation. This data indicates the potential of capturing vehicle-generated wind energy for electric power generation, which could help California meet its clean energy goals and mitigate the negative impacts of climate change.

| 17. Key Words<br>Large-eddy simulation, Turbulent shear, Aerodynamics, Vehicle's drag, Fluid-structure interaction | 18. Distribution Statement<br>No restrictions. This document is available to the public through The National Technical Information Service, Springfield, VA 22161. | | |
|---|---|---|---|
| 19. Security Classif. (of this report)<br>Unclassified | 20. Security Classif. (of this page)<br>Unclassified | 21. No. of Pages<br>30 | 22. Price |

Form DOT F 1700.7 (8-72)

Copyright © 2022

by **Mineta Transportation Institute**

All rights reserved.

DOI: 10.31979/mti.2022.2145

Mineta Transportation Institute
College of Business
San José State University
San José, CA 95192-0219

Tel: (408) 924-7560
Fax: (408) 924-7565
Email: mineta-institute@sjsu.edu

transweb.sjsu.edu/research/2145

# ACKNOWLEDGMENTS

# CONTENTS

# LIST OF FIGURES

# Executive Summary

Wind generated from passing vehicles on roads and freeways is wasted energy. Harnessing this energy adds to California's renewable energy portfolio for various commercial and transportation-related applications. We investigated the transient wind and load generated from passing vehicles under a freeway overpass to check its viability for electric power generation.

As California moves toward a 100% clean energy future, expanded wind energy will be a major component of its future energy portfolio, and innovations in wind energy resources will move the state closer to achieving its goal. California is also the first U.S. state to set a goal of banning the sale of new internal combustion engines or gas-powered vehicles by 2035. Because the transportation sector is responsible for nearly 50% of the state's greenhouse gas emissions, this goal aims to significantly increase the number of electric vehicles within California. With a $1.2 billion investment in electric vehicles and charging stations, the California Electric Vehicle Infrastructure Project (CALeVIP) intends to meet the region's needs for electric vehicle charging infrastructure.

Investments in infrastructures have increased significantly, including funding through the California Senate Bill 1 (SB1) and the federal government's $1 trillion infrastructure bill. The incorporation of structural health monitoring sensors allows for continuous inspection, maintenance, and detection of any infrastructure damages, and these sensors all require remote electric power sources to operate. Local power generated from passing vehicles may provide power for sensors, vehicle-charging stations, and other energy needs.

In this study, we performed large eddy simulations of a vehicle passing under a freeway overpass in order to identify wind energy potential at the bridge columns with the vehicle moving at 51.5 mph. The distance between the bridge column and the vehicle was 0.75 W where W is the width of the vehicle. Results indicate a transient wind of 6-10 m/s with a maximum pressure coefficient differential of 0.17 around the bridge columns from the passing vehicle. With the high volume of traffic on California's highways and roads, these results indicate great potential for generating electricity from passing vehicles.

# 1. Introduction

Wind generated from passing vehicles is related to shape and pressure distributions around the vehicle, and around a moving vehicle, there are various pressure zones. High-pressure zones can be found in front of the vehicle at the stagnation points; reduced-pressure zones with flow acceleration from the stagnation point are in front of the vehicle toward the rear of the vehicle; zones of relatively constant pressure are at the top and bottom of the vehicle; flow separation zones are in the rear with negative pressure in the near wake and ambient pressure in the far wake due to pressure recovery. The transient pressure induces loads on objects on the sides and above the vehicle.

A detailed experimental investigation [1] of the wind-load generated by vehicles on road signs has shown that the force acting on these signs during the passage of a vehicle differs with respect to the vehicle's aerodynamics and the sign's location. The highest force on the road sign is imposed by the front of the vehicle, and the load amount depends on the distance between the vehicle and the sign. Depending on the force amplitude and its duration, the impact on the road sign could result in dynamic reactions and material fatigue. The investigations included various-sized vehicles and three road signs with different areas. Two signs had areas perpendicular to the vehicle's direction (one on the side and one on top), and for the third sign, the area was aligned with the vehicle's direction. The pressure was significantly higher on the third sign and peaked in the positive direction ahead of the approaching vehicle and decreased to a negative value with the passage of the lead vehicle area. Here, the suction pressure is not as low as in the other cases due to air movements around the sign.

Other investigations [2–9] into the load induced on road signs and vehicle-induced gusts have provided similar results with additional details of wind profiles around the vehicles. A study [10] on the effect of natural wind on road signs has shown a reduced mean drag coefficient as compared to the corresponding value published by the American Association of State Highway and Transportation Officials (AASHTO) with its variations depending on the aspect and depth ratio of the sign.

Turbulent flow-inducing force on road signs [1] has mean and fluctuating components given as:

$$\bar{F} = \frac{1}{2}\rho\overline{u_w}^2 A C_w$$

$$\acute{F} = \frac{1}{2}\rho\overline{u_w}\acute{u}_w A C_w$$

Here $\bar{F}$ and $\acute{F}$ are mean and fluctuating forces; $\rho$ and $A$ are air density and area of the sign, respectively; $\overline{u_w}$ and $\acute{u}_w$ are mean and fluctuating wind velocity, respectively; and $C_w$ is a constant relating the wind pressure to the force exerted on the road signs. When the signs are away from the ground, the non-linear effect (the ground effect) is not significant and there is a linear

relationship between the wind pressure and the force exerted. However, when the signs are within a few meters of the ground, the relationship becomes non-linear, and its impact should be considered in calculating the force exerted.

Nonlinearity is related to the size of the fluid eddies approaching the sign. Previous investigations [11, 12] have shown that when the fluid integral length scale L is much larger than the size of the object D, L/D >> 1, the velocity intensity is decreased, and the energy distribution of the spectral axial turbulent velocity is unchanged. However, when L/D << 1, the velocity intensity is increased near the object due to vortex stretching, which results in amplification and attenuation of spectral values at respectively low and high wavenumbers. Thus, when the road signs are within a few meters of the ground within the atmospheric boundary layer, the size of the incoming eddies changes, and the ground causes a breakdown of the eddies, reducing their sizes as compared to the road signs, resulting in increased turbulence intensity as the wind approaches the signs.

In the wake of the objects, previous investigation [13] has shown that when L/D >> 1, the momentum transport from the free stream into the wake is increased, resulting in reduced mean defect velocity, maximum turbulent shear stress, and increased wake half-width. However, for L/D << 1, the wake is unchanged. These characteristics affect the vehicle's drag as the drag coefficient is mostly pressure drag, and if the base pressure is not affected, then the drag coefficient is unchanged.

Recent unsteady numerical simulations of an Ahmed body under a freeway overpass [14] have shown that when the vehicle is at a distance of 0.75w from the bridge column, where w is the width of the vehicle, gusts of up to 23 m/s (51.5 mph or 82.4 km/h) are generated near the bridge column. In this region, the turbulent kinetic energy and vorticity are reduced indicating less fluctuations in the wind-generated. On the top of the vehicle near the end, the wind speed is higher than 24 m/s, which decreases downstream. As the vehicle passes the columns, in the vehicle's wake, vortices are increased and expanded, and the turbulent kinetic energy is amplified.

The present investigation is an extension of our previous study [14] with more focus on the transient nature of the wind and load on and around freeway overpass columns. The same Ahmed body was used as the vehicle, and the distance between the vehicle and the columns was 0.75w. Details of transient mean pressure and velocity, vorticity, and turbulent kinetic energy are provided. The impact of the bridge columns on the flow around the vehicle and between the vehicle and the columns has also been investigated.

# 2. Numerical Investigations

Numerical investigations were performed using an Ahmed body. The dimensions for a freeway overpass were set according to a typical freeway overpass on the I-405 freeway near Long Beach, California.

## 2.1 The Ahmed Body and the Overpass Bridge

Figure 1 shows the Ahmed body used in the numerical simulations, which has dimensions of 1.62 m in height, 5 m in length, and 1.86 m in width. The hatchback's rear starts at 4.14 m from the front at a 35-degree angle. The vehicle is spaced at 0.28 m above the ground. The size of the vehicle represents a typical mid-sized sport utility vehicle (SUV).

Figure 1. The Ahmed Body
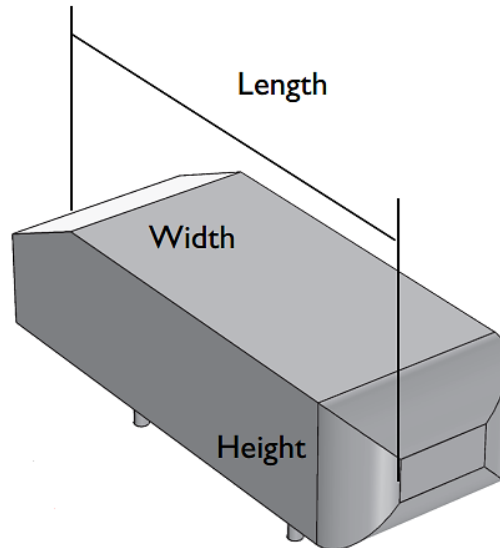


Figure 2 shows different views of the bridge columns with the Ahmed body. The computational domain that encompasses the freeway overpass has dimensions of X = 30 m, Y = 11.25 m, and Z = 14.5 m with a grid size of 0.85 cm. Here, X is the direction of the moving vehicle, and Y and Z are vertical and spanwise directions, respectively. The distance between the vehicle and the freeway bridge columns is 0.75W. Here W is the width of the vehicle. The bridge has six cylindrical columns equally spaced with a diameter of 1.34 m, and the spacing between the columns was 2.46 m.

An overset grid technique (moving mesh) was used for the moving vehicle, with an overset region of 8 m x 3.5 m x 6 m in the X, Y, and Z directions, respectively. The blockage ratio was less than 3%.

Figure 2. The Bridge Columns and the Computational Domain
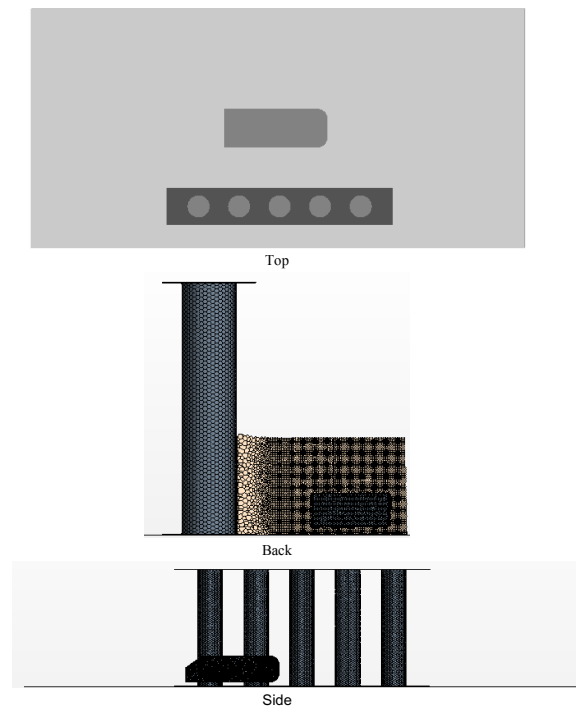


## 2.2 Simulations

A hybrid mesh with an unstructured polyhedral grid away from the wall and a structured 15 layers hexahedral grid near the wall was used. The first grid cell size near the Ahmed body was at 0.0025 mm with a surface growth rate of 1.0. The far-field grid cell size was at 0.005 m. The maximum grid size was calculated using the following equation:

$$\text{Grid size} = \text{growth rate} \times R_{eH}^{\frac{7}{8}}$$

Here $R_{eH}$ is the Reynolds number based on the height of the vehicle. The total cells used for the computation was 40,796,718 with the overset cell numbers at 14,182,797.

Figure 3. The Computational Mesh
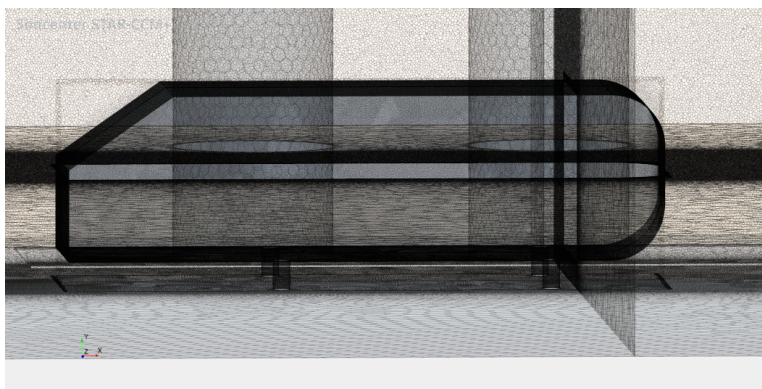


The vehicle's velocity was 23 m/s (51.5 mph), which corresponds to a Reynolds number based on the vehicle's height of $2.4 \times 10^6$.

Figures 4 and 5 show the vehicle's locations with respect to the bridge columns at different time steps and the monitoring column, which is the center column. The vertical direction is the direction of pressure measurements on the column, and the horizontal direction is where circumferential pressure measurements were made. It also corresponds to the mid-section plane of the vehicle in the spanwise direction.

Figure 4. Vehicle Location at Different Time Steps
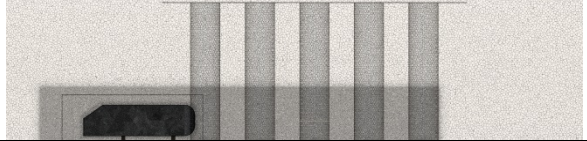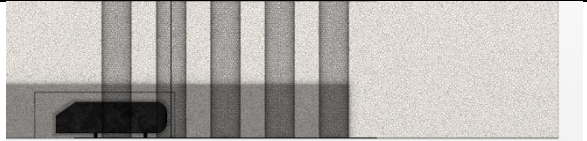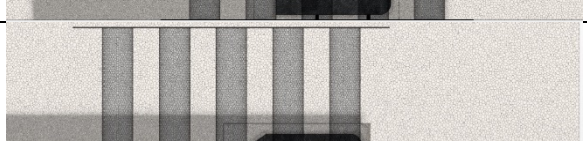
| Time (s) | Vehicle Location |
|----------|------------------|
| 0.04 |  |
| 0.16 |  |
| 0.27 |  |
| 0.30 |  |
| 0.40 |  |
| 0.50 |  |

Figure 5. The Reference Column and Measurement Locations

| Vertical | Spanwise |
|----------|----------|
|  |  |
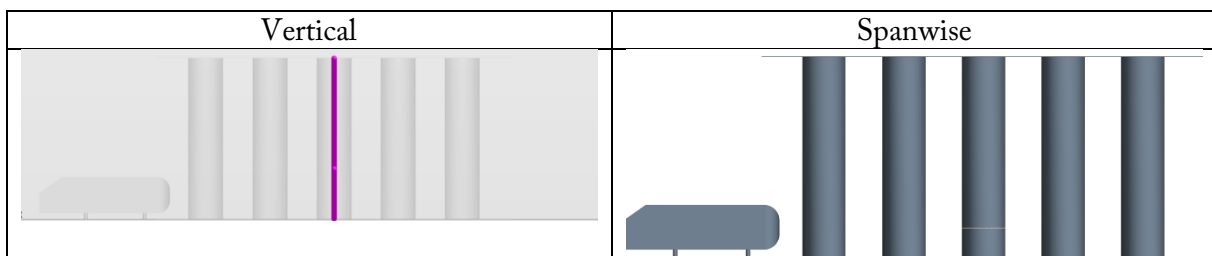
# 3. Results and Discussion

Figures 6 and 7 show contours of mean pressure and velocity at four-time steps of 0.1 s, 0.2 s, 0.3 s, and 0.5 s. These time steps correspond to the vehicle's location with respect to the bridge columns, where a middle column is taken as the monitoring column. The contours correspond to the mid-section plane of the vehicle. For all time steps, pressure is at its highest at the front stagnation points of the vehicle and decreases and becomes negative along the side of the vehicle. The wake characteristics change at different time steps. At 0.1 s, the pressure recovery occurs at about 0.2 W and is maintained up to more than 1 W before it decreases to atmospheric pressure. At 0.2 s, the region of pressure recovery is narrowed and extended downstream. On each side of the wake's high-pressure region, there are two areas of positive and negative pressures which correspond to enhanced wake vortices in these regions.

At 0.3 s, the wake has been expanded with increased areas of positive and negative pressures on the sides and a reduced area of pressure recovery in the middle. At 0.5 s, the side columns impose a pressure gradient on the side of the vehicle, creating an asymmetric pressure distribution in the wake. The area of pressure recovery in the middle has been reduced further with the location of the pressure recovery being further away from the vehicle. The reduced pressure recovery should result in increased vehicle drag.

Figure 6. Contours of the Pressure Coefficient Around the Vehicle
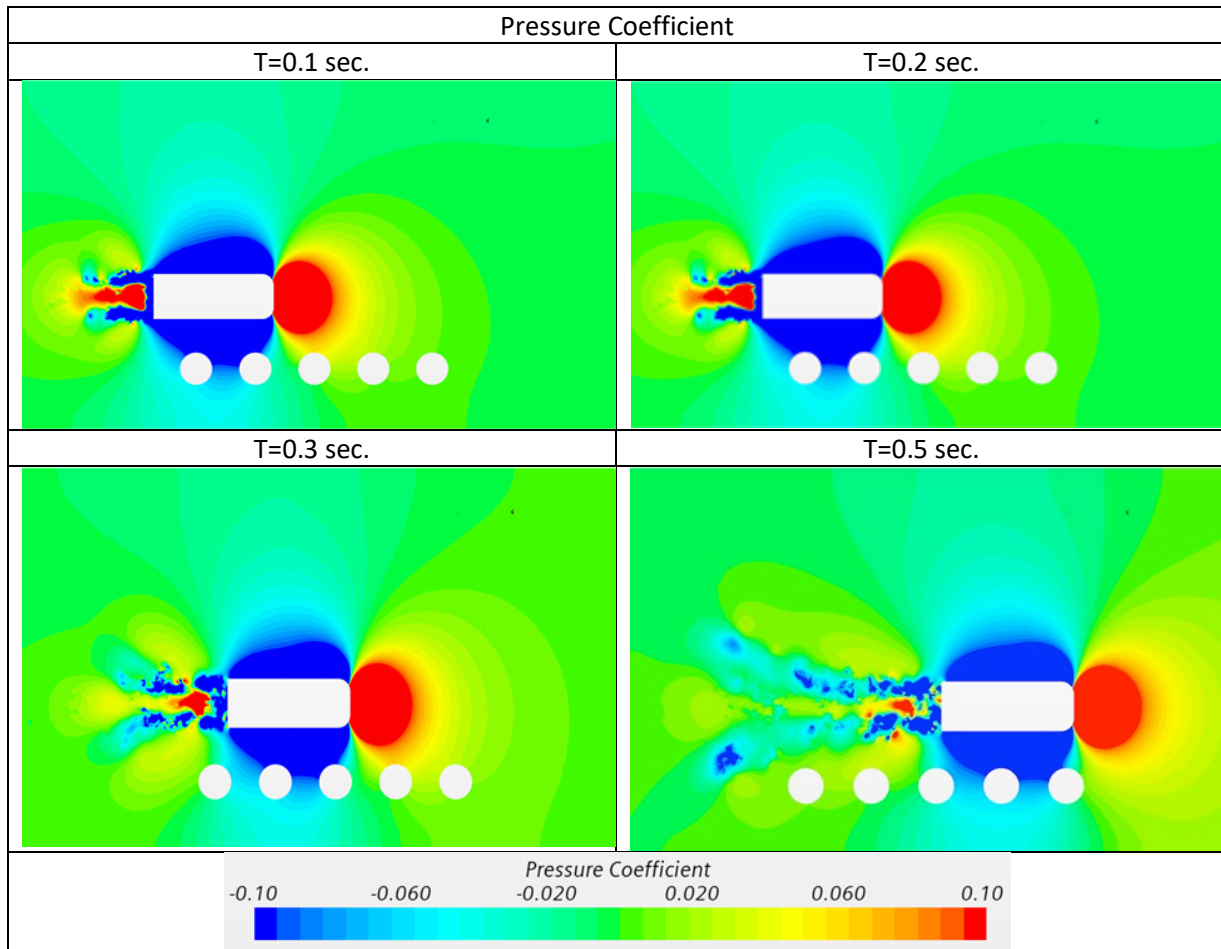


The behaviors of the mean velocity contours are in opposition to the corresponding mean pressure contours, with zero velocity in the front at the stagnation points, acceleration on the vehicle's side, and then separation at the rear, shedding vortices into the wake. Increased shedding and unsteadiness are observed as the vehicle passes the columns. The columns experience a transient mean velocity of around 6 m/s as the vehicle approaches.

Figure 7. Contours of Mean Velocity Around the Vehicle
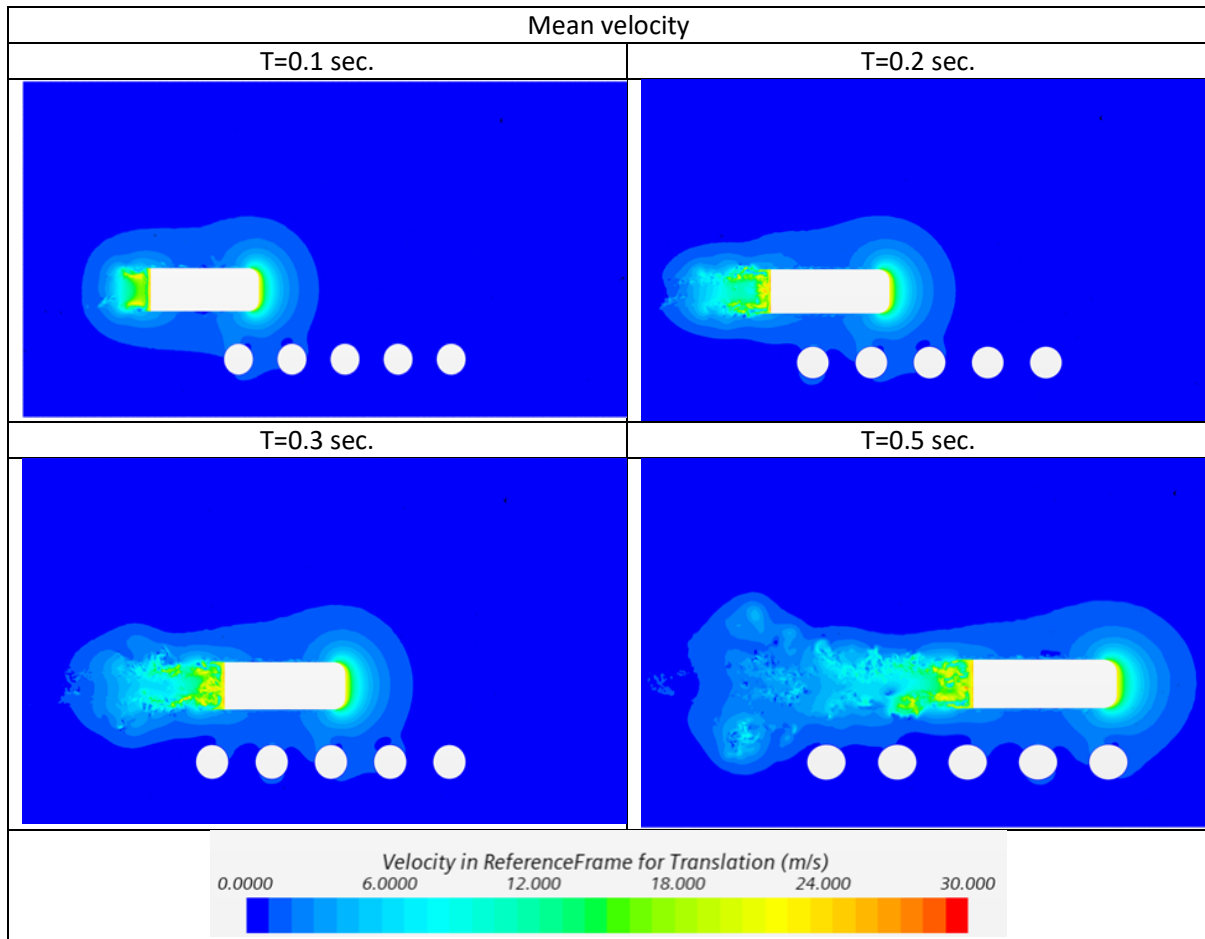


The columns experience a high-pressure coefficient of approximately 0.02 as the vehicle approaches, a negative pressure coefficient of -0.1 when the columns face the vehicle's side, and an increased pressure coefficient of around 0.02 from the vehicle's wake [Figure 8].

Figure 8. Contours of the Mean Pressure Coefficient Around the Referenced Column
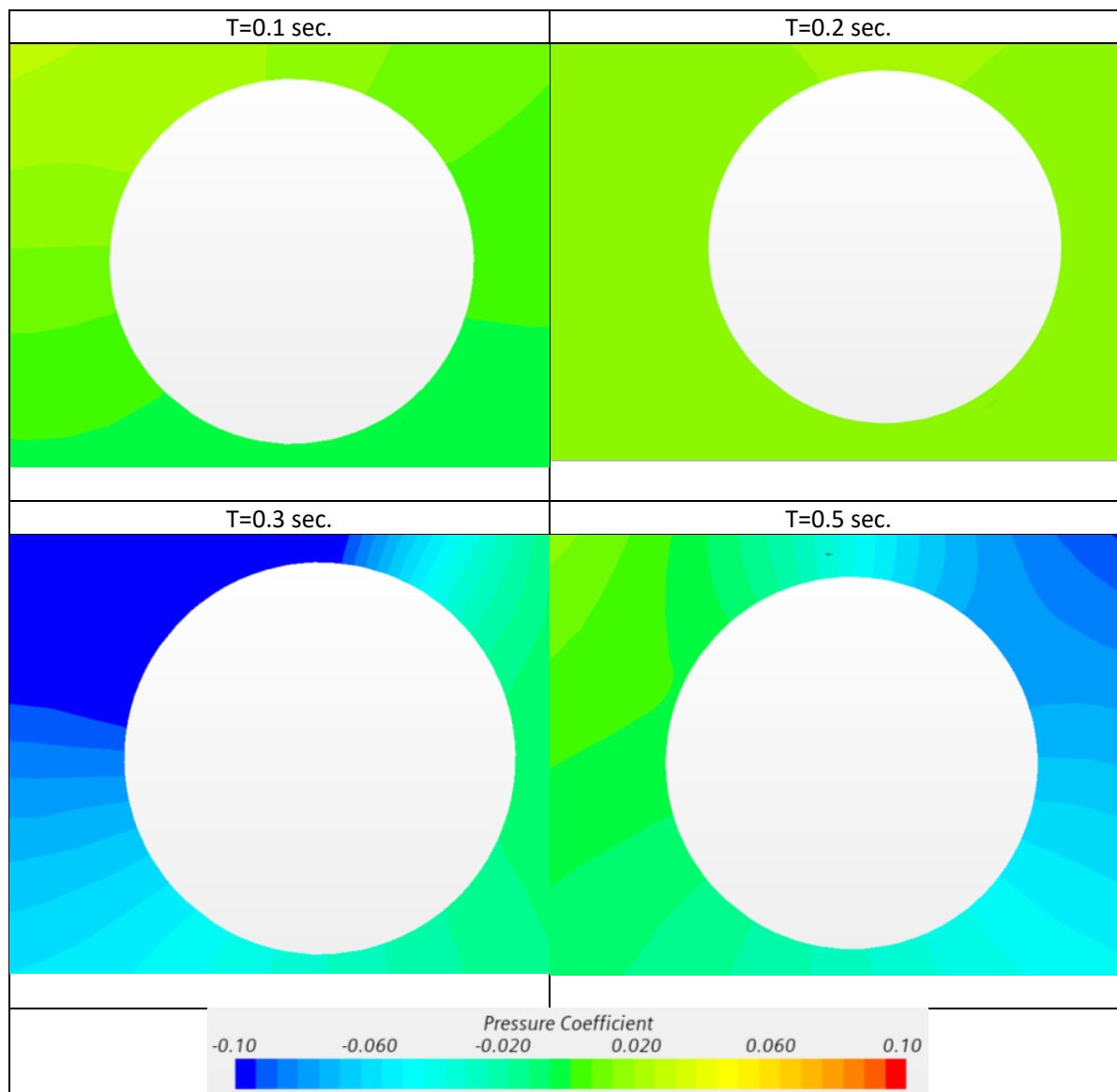


Figures 9 and 10 show contours of mean vorticity and turbulence kinetic energy (TKE) at different time steps. Vorticity is high in the wake due to the unsteady flow separation. The wake vortices are enhanced with the passage of the vehicle adjacent to the columns.

The TKE is high around the vehicle and in the wake. With the passage of the vehicle near the columns, the areas around and downstream of the vehicle with high TKE are narrowed, and the wake with high TKE is extended. These areas correspond to the areas with increased vortices.

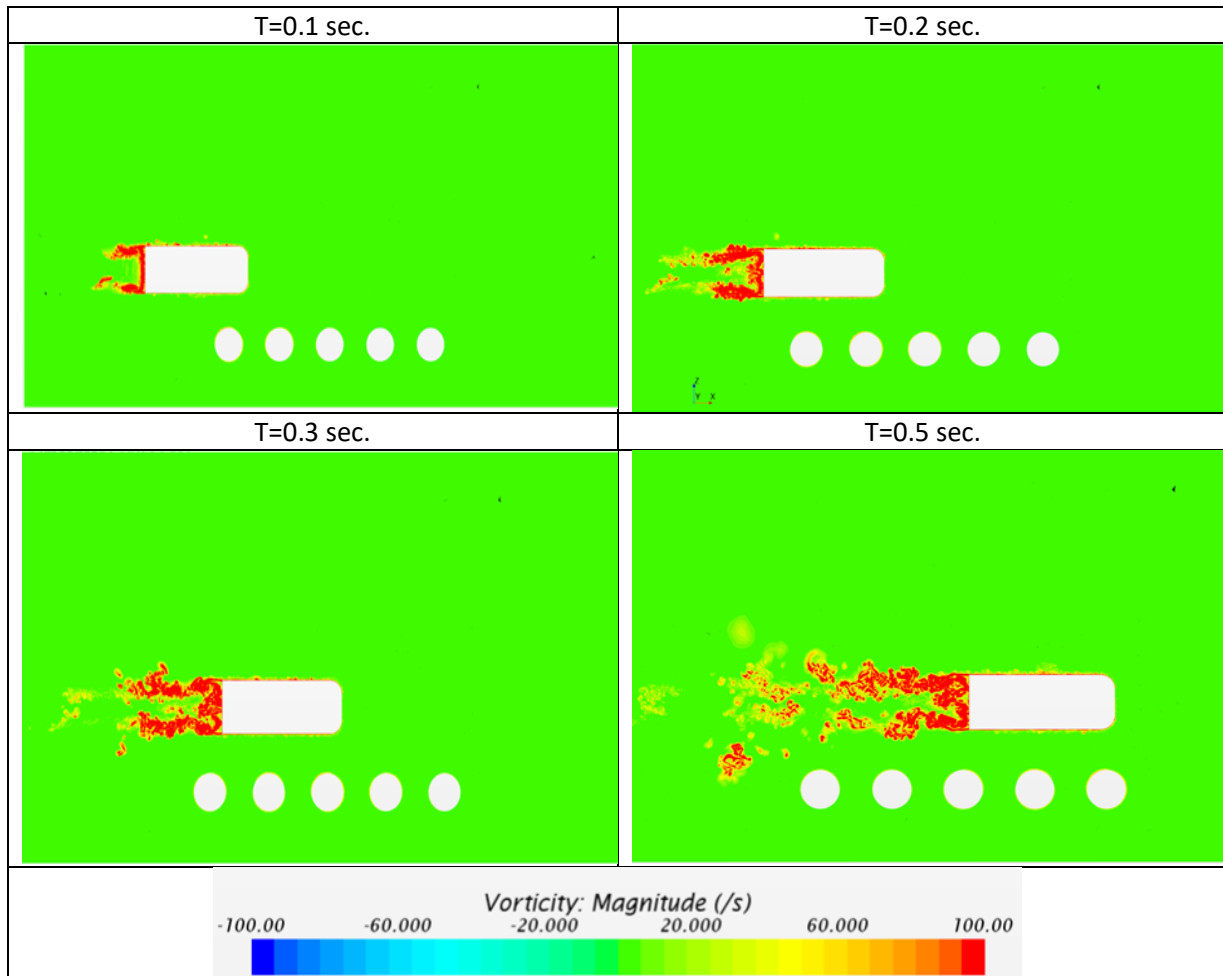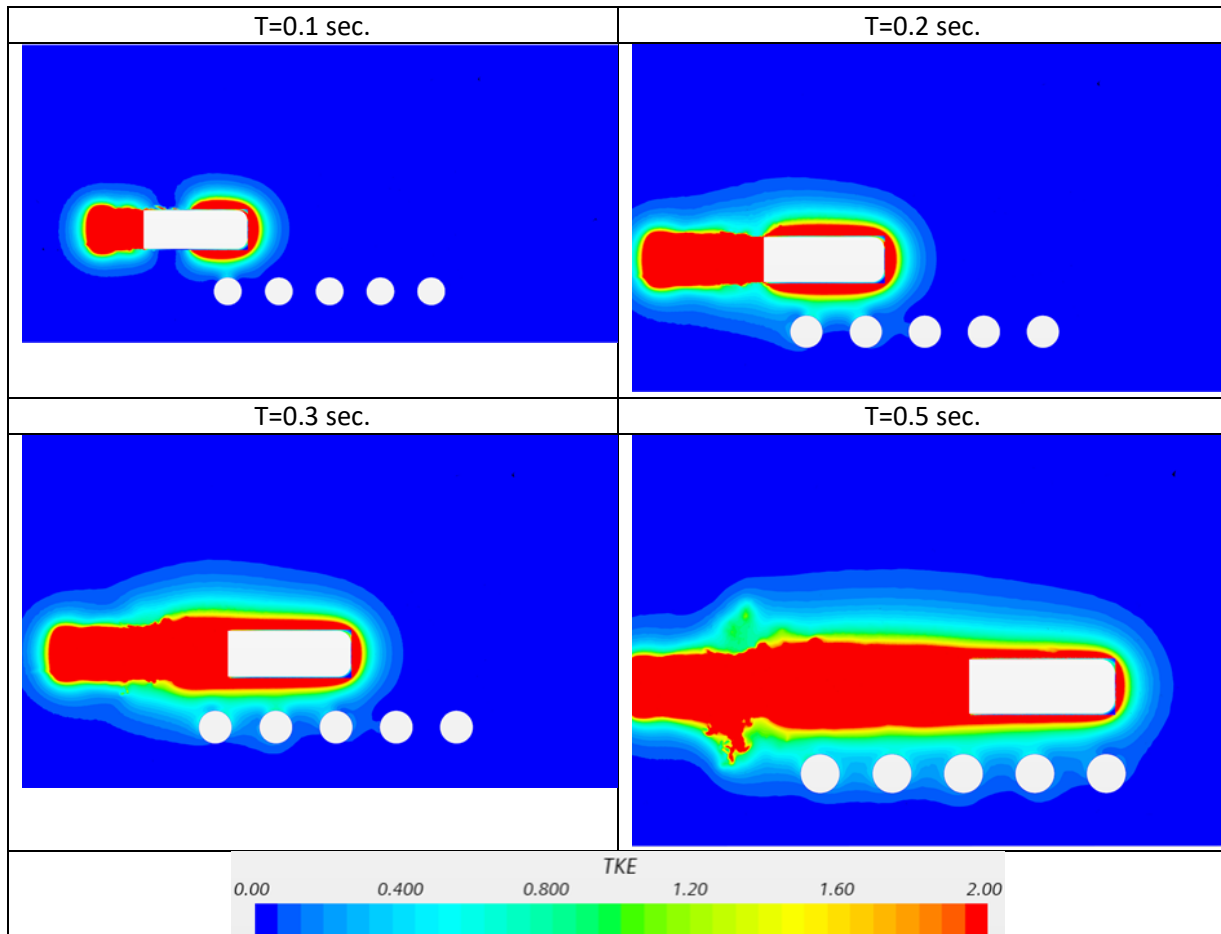Figure 9. Contours of the Mean Vortices Around the Vehicle

Figure 10. Contours of the Turbulent Kinetic Energy (TKE) Around the Vehicle



The vortices and TKE have limited impacts on the columns.

Figures 11 and 12 show variations of circumferential and vertical pressure coefficients at different time steps for the referenced column. For the circumferential pressure coefficient, zero degrees is at the front of the column, and pressure data was taken in a counter-clockwise direction. For the vertical data, zero Y corresponds to the mid-level of the vehicle, and data was collected from the ground up.

With the approaching vehicle, at T = 0.1 s, the circumferential pressure coefficient peaks at 0.042 at 140 degrees and reduces to 0.007 at 272 degrees before increasing to 0.02 at 360 degrees. At T = 0.2 s, the pressure is increased, and the peak pressure is 0.055 at 112 degrees with a minimum pressure coefficient of -0.01 at around 200 degrees.

The pressure variation changes with the passage of the vehicle. At T = 0.3 s, the pressure coefficient drops to -0.14 at 117 degrees, before it increases to near zero at 360 degrees. At T = 0.5 s, there is an initial drop in pressure coefficient from -0.075 at 0 degrees to -0.08 at around 45 degrees before

it increases to near zero at 150 degrees, and then drops again to a minimum of -0.075 at 360 degrees. The maximum difference in circumferential pressure coefficient, the column experiences with the passage of the vehicle is 0.2 over 0.5 s.

Figure 11. Variation of the Circumferential Pressure Coefficient
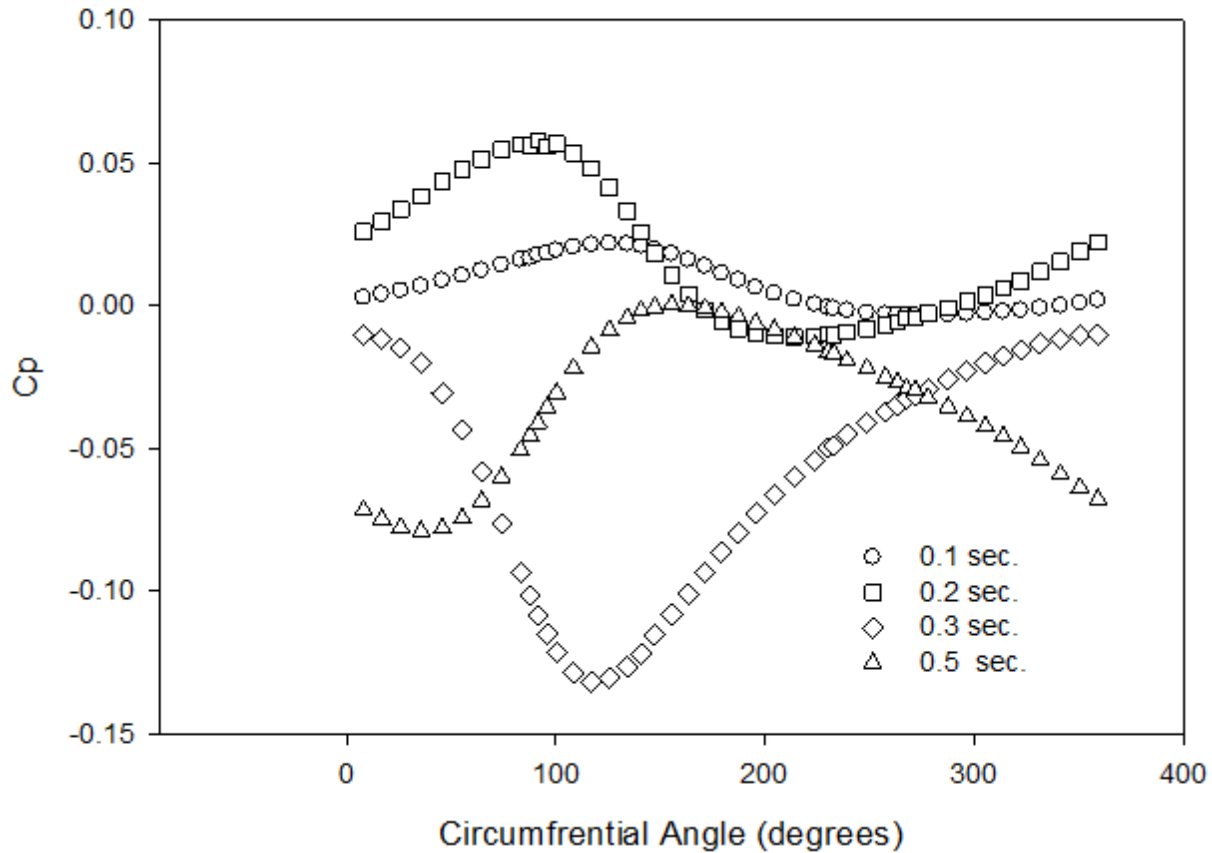


The vertical pressure was obtained along 90 degrees angle from the ground-up. Here y = 0 corresponds to the mid-section elevation of the vehicle. At T = 0.1 s, there is an increase in pressure near the ground that decreases in the vertical direction. At T = 0.2 s, the pressure is doubled near the ground and approaches zero at y > 4 m. However, for T = 0.3 s, the variation of the pressure coefficient changes significantly and is -0.105 near the ground and decreases to -0.04 at y = 3 m. At T = 0.5 s, the pressure coefficient is -0.04 near the ground, decreasing further to -0.05 at around y = 2.5 m before it decreases to -0.26 at y = 3 m. The total difference in pressure coefficients as the vehicle passes the column over 0.35 s is 0.17.

Figure 12. Variation of the Vertical Pressure Coefficient
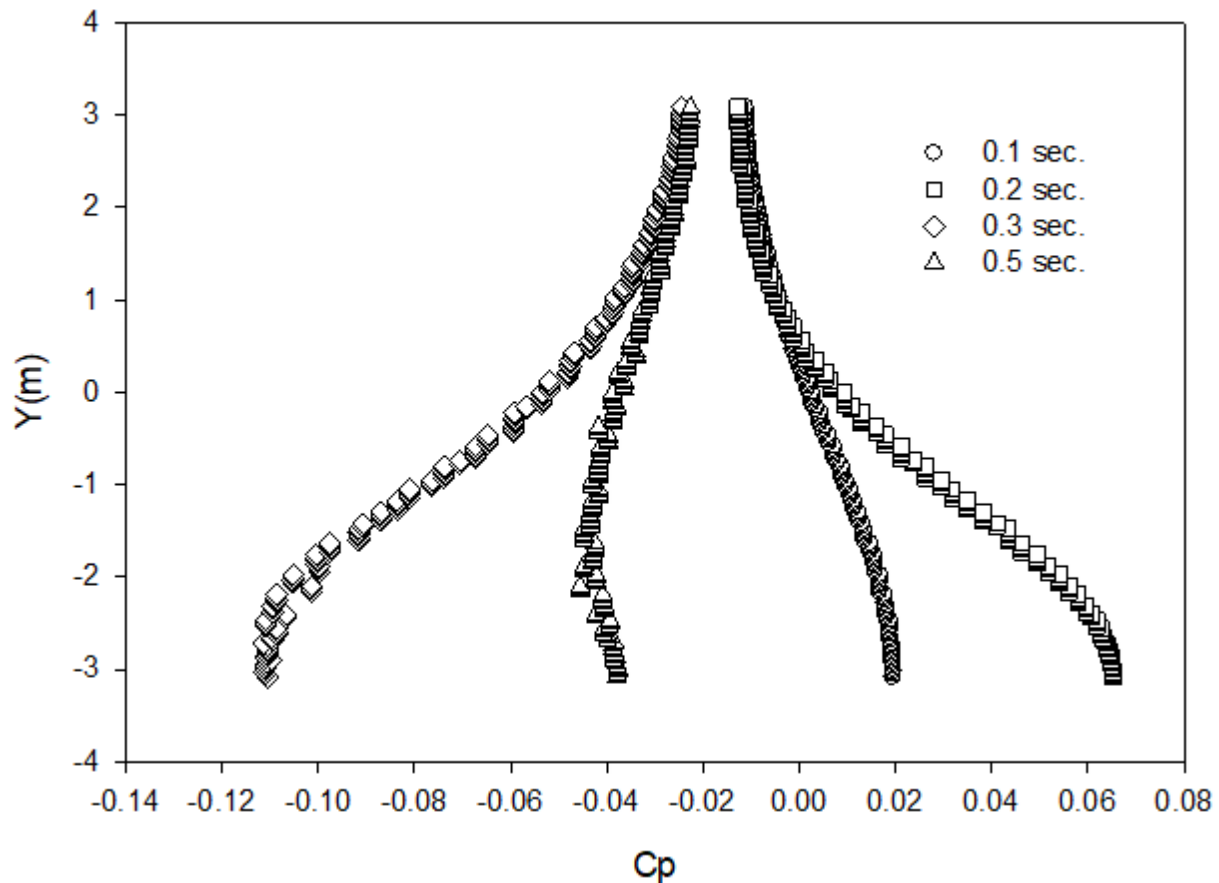


Figures 13 and 14 show variations of the pressure coefficient at the mid-section vertical plane and the back of the vehicle at different time steps. The pressure coefficient is 1 at the front stagnation point, decreases with flow acceleration, and becomes a minimum of approximately -1.67 at X = 0.4 m, before it increases due to flow deceleration and approaches a constant value of -0.125 at X = 1.7 m. The pressure coefficient decreases starting at X = 4.2 m which corresponds to the start of the slanted section of the vehicle, and the minimum pressure is different at different times, which means the drag coefficient could be transient. At T= 0.1 s, the minimum pressure is -1.85 at X = 4.275 m while the corresponding values at T = 0.2 s, 0.3 s, and 0.5 s are -1.3 at X = 4.34 m, -1.58 at X = 4.32 m, and -1.2 at X = 4.3 m, respectively. Considering the location of the vehicle (Figure 4), the effect of the columns is seen as increasing axial momentum at the mid-section plane, resulting in increased minimum pressure.

Variations of the back pressure coefficient are different at different locations (time steps). At T = 0.3 s and 0.5 s, the constraints imposed by the columns on the vehicle are significant, resulting in a faster pressure recovery. The increased pressure recovery should result in a reduced drag coefficient. However, the imposition of constraints by the columns also has increased three-dimensionality in the wake of the vehicle.

Figure 13. Variation of the Pressure Coefficient on the Top of the Vehicle at the Axial Mid-section Plane
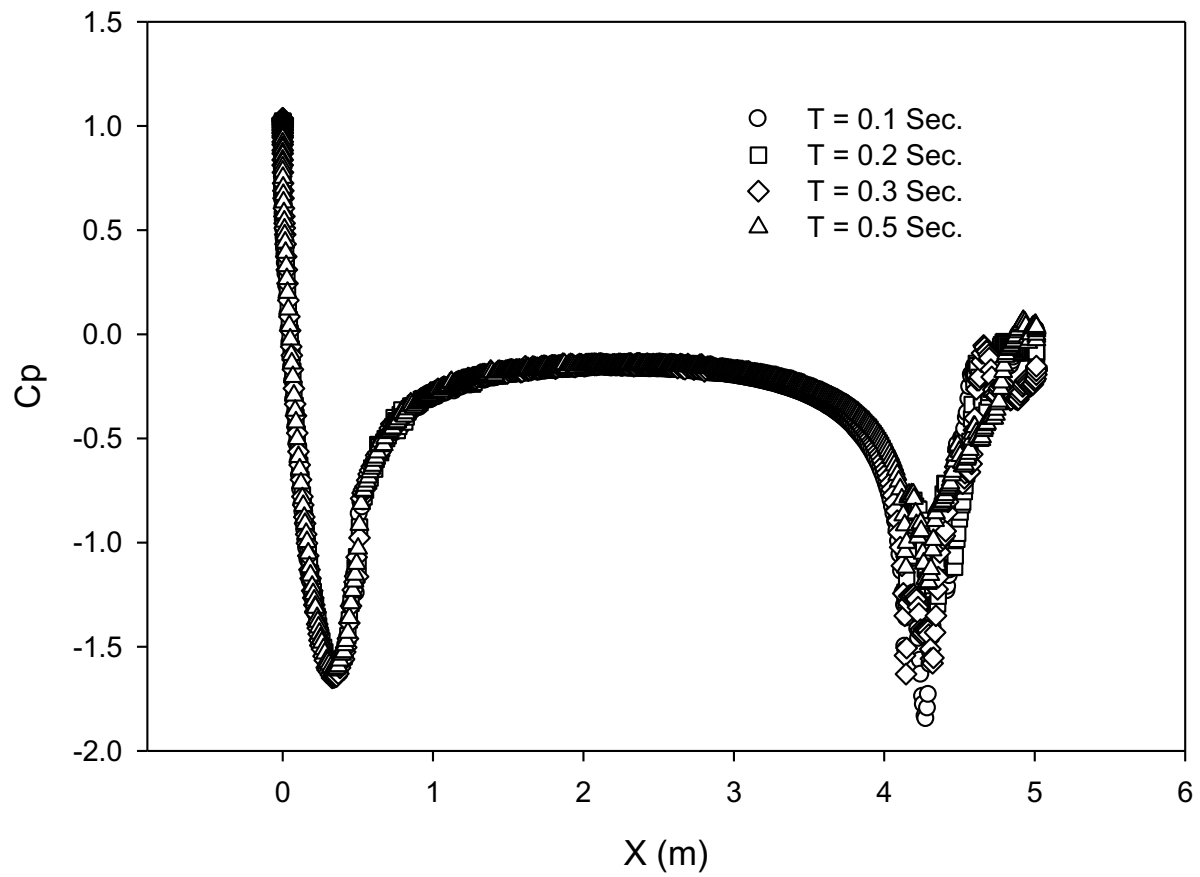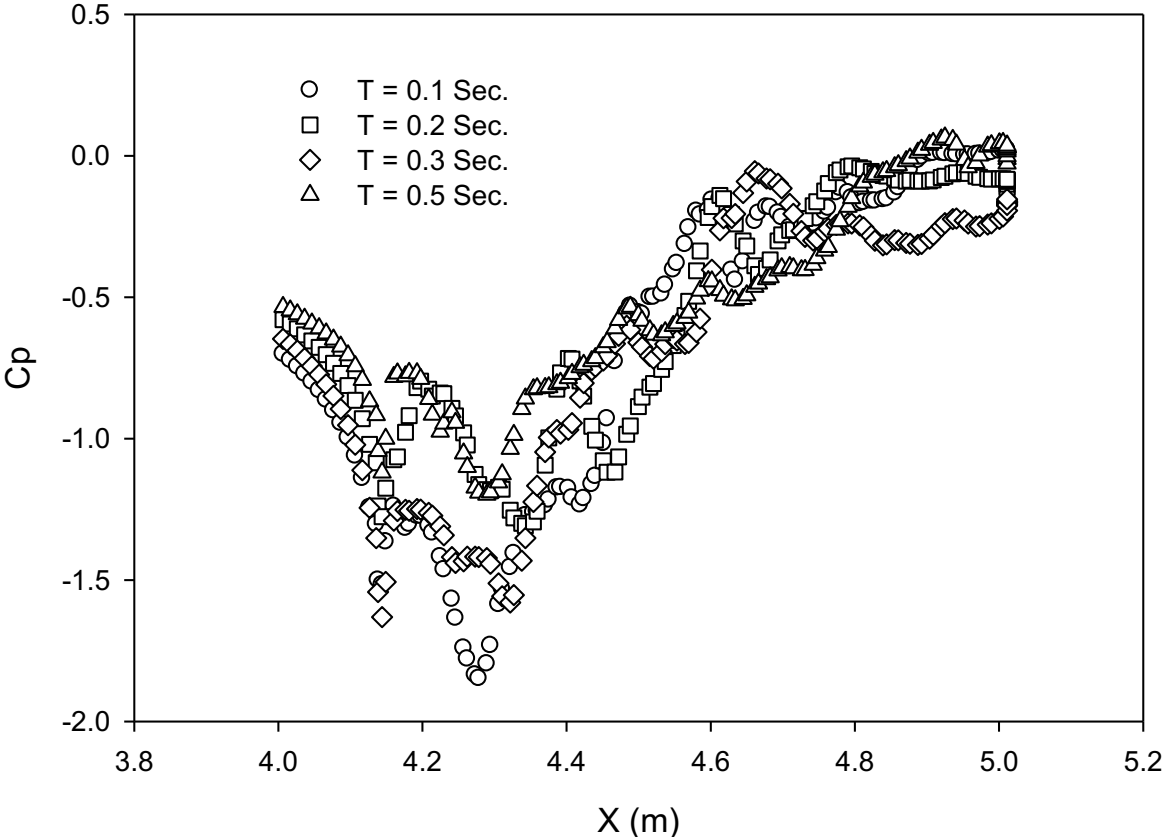
Figure 14. Variation of the Pressure Coefficient at the Back of the Vehicle

# 4. Summary & Conclusions

Large eddy simulations of a vehicle passing under a freeway overpass near freeway columns were performed to gain a better understanding of the transient wind and pressure distribution characteristics at the bridge columns for potential electric power generation. The vehicle was an Ahmed body traveling at 23 m/s (51.5 mph) at 0.75 W from the bridge columns. Here, W is the width of the vehicle. Results show that the bridge constraints cause changes in the baseline vehicle pressure which affects the transient vehicle's drag coefficient. The transient wind generated at the columns is mostly caused by the front of the vehicle and ranged from 6 m/s to 10 m/s. The circumferential pressure distributions on the referenced column show that the stagnation point changes with the passing of the vehicle with a maximum differential pressure coefficient of 0.2. The ground effects are seen up to 5 m elevations where the pressure coefficient changes from positive to negative from the passing of the vehicle with a maximum difference of 0.17. Using a high-efficiency vertical axis wind turbine with a 0.35 power coefficient, the potential for power generation at the bridge columns from passing a vehicle is approximately 210 W/m². With continuous traffic flow, significant electric power could be generated from the passing of the vehicles.

# References

1. Lichtneger, P. and Ruck, B. "Full Scale Experiments on Vehicle Induced Transient Loads on Roadside Plates." *J. Wind Eng. Ind. Aerodyn.* 136 (2015), 73-81.

2. Ruck, B. and Lichtneger, P. "Wind Loads on Flat Board and Walls Induced by Passing." *Fachtagung: Lasermethodyn in der Strömungsmesstechnik* (September 2014). https://gala-ev.org/images/Beitraege/Beitraege%202014/pdf/14.pdf.

3. Salvadori, S., Morbiato, T., Mathana, A., and Fusto, E. "On the Characterization of Wind Profile Generated by Road Traffic." In *Seventh International Collequium on Bluff Body Aerodynamics and Applications (BBAA7*, 1729–1741. Shanghai, China: September 2012.

4. Sanz-Andres, A., Santiago-Prowald, J., Baker, C., and Quinn, A. "Vehicle-Induced Loads on Pedestrian Barriers." *J. Wind Eng. Ind. Aerodyn.* 92 (2003): 413-426.

5. Sanz-Andres, A., Laveron, A., and Quinn, A., "Vehicle-Induced Loads on Traffic Sign Panels." *J. Wind Eng. Ind. Aerodyn.* 91 (2003): 925-942.

6. Quinn, A.D., Baker, C. J., and Wright N. G. "Wind and Vehicle Induced Forces on Flat Plates-Part I: Wind Induced Forces." *J. Wind Eng. Ind. Aerodyn.* 89 (2001): 811–823.

7. Quinn, A.D., Baker, C. J., and Wright N. G. "Wind and Vehicle Induced Forces on Flat Plates-Part II: Vehicle Induced Forces." *J. Wind Eng. Ind. Aerodyn.* 89 (2001): 831–847.

8. Cali, P. M., and Covert E. E.. "Experimental Measurements of the Loads Induced on an Overhead Highway Sign Structure by Vehicle-Induced Gusts." *J. Wind Eng. Ind. Aerodyn.* 84 (2000): 87-100.

9. Zou, Y., Fu, Z., He, X., Cai, C., Zhou, J., and Zhou, S. "Wind Load Characteristics of Wind Barriers Induced by High-Speed Trains Based on Field Measurements." *Appl. Sci.* 9 (2019), 4865. doi:10.3390/app9224865.

10. Meyer, D., Zisis, I, Hajra, B., Chawdhury, A.G., and Irwin, P. "An Experimental Study on the Wind-Induced Response of Variable Message Signs." *Frontiers in Build Environment* Vol. 3 (2017), Article 66.

11. Rahai, H. R. and LaRue, J. "The Distortion of a Passive Scalar by Two-Dimensional Objects." *Phys. Fluids,* 7 (1995), no. 1, 98-107.

12. Rahai, H. R. and LaRue, J. "Distortion of a Turbulent Scalar Upstream of Axi-symmetric Objects." *AIAA J. of Thermophysics and Heat Transfer* 7 (1993), no. 3, 524-526.

13. Rahai, H.R. and LaRue, J. "Decay of Temperature Variance in the Presence of Non-Homogenous  Strain." *ASME J. of Fluids Engineering* 114 (1992), 155-160.

14. Rahai, H. and Begum, A. "Numerical Investigations of Transient Wind Shear from Passing Vehicles near a Road Structure." *SAE Technical Paper* 2021-01-0964. doi:10.4271/2021-01-0964.

# About the Authors

**Hamid Rahai, Ph.D.**

Dr. Rahai is a Professor in the Departments of Mechanical and Aerospace Engineering & Biomedical Engineering and Associate Dean for Research and Graduate Studies in the College of Engineering at California State University, Long Beach (CSULB). He has supervised over 70 Master's theses, projects, and PhD dissertations and published more than 90 technical papers. He has received over $11 million in grants and contracts from the National Science Foundation, Federal Highway Administration, California Energy Commission, California Air Resources Board, Port of Los Angeles, California Department of Transportation (Caltrans), The Boeing Company, Southern California Edison, Long Beach Airport, and Long Beach Transit, among others. He has been granted patents for a high-efficiency vertical axis wind turbine (VAWT) and wind turbine apparatus and for reducing NOx emission of Cargo Handling Equipment using a Humid Air System. He also has pending patents related to a new conformal vortex generator tape for reducing wing-tip vortices, and environmental artificial trees for reducing ambient NOx. For the past 26 years, he has been a consultant to the local energy and aerospace industries. Dr. Rahai is the recipient of several scholarly and creative activities awards (RSCA), including the 2012 CSULB Impact Accomplishment of the Year in RSCA Award, the 2002–2003 CSULB Distinguished Faculty RSCA Award, and the 2004 Northrop Grumman Excellence in Teaching Award. Dr. Rahai received the Outstanding Engineering Educator Award from the Orange County Engineering Council in California in 2014, and in 2019, he was inducted as a senior member of the National Academy of Inventors (NAI).

**Assma Begum, M.S.**

Assma is a graduate student in the joint Ph.D. program in Engineering and Computational Mathematics between CSULB's College of Engineering and the Claremont Graduate University (CGU) and a research assistant at the Center for Energy and Environmental Research & Services (CEERS) in the College of Engineering at CSULB. She has been involved in various projects at CEERS related to the aerodynamics of rotating cylinders and wind shears from passing vehicles. Assma is the author and co-author of two technical conference papers and one journal paper.

**MTI** // **MINETA TRANSPORTATION INSTITUTE**